

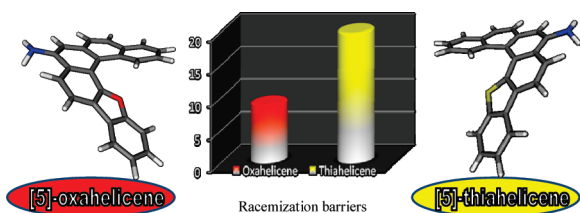
**Regio-Defined Amino[5]Oxa- and Thiahelicenes:
A Dramatic Impact of the Nature of the Heteroatom
on the Helical Shape and Racemization Barriers**

Grégory Pieters,[†] Anne Gaucher,^{*†} Sylvain Marque,[†]
François Maurel,[‡] Philippe Lesot,[§] and Damien Prim^{*†}

[†]Institut Lavoisier de Versailles, UMR CNRS 8180,
Université de Versailles-Saint-Quentin-en-Yvelines, 45,
Avenue des Etats-Unis, 78035 Versailles cedex, France,
[‡]Interfaces, Traitements, Organisation et Dynamique des
Systèmes (ITODYS), UMR CNRS 7086, Université Paris
7-Paris Diderot, Bâtiment Lavoisier, 15, rue Jean Antoine de
Baïf, 75205 Paris, France, and [§]RMN en Milieu Orienté,
ICMMO, UMR CNRS 8182, Université Paris Sud 11,
Bâtiment 410, 91405 Orsay cedex, France

gaucher@chimie.uvsq.fr; prim@chimie.uvsq.fr

Received January 6, 2010



The present approach to heterohelicenes provides original [5]oxa- and thiahelicenes, where both oxygen and sulfur atoms are located at the end of the inner helix. Quantum chemical calculations are carried out to determine the pathway for interconversion between two enantiomers and demonstrate that the energy barrier is strongly dependent on the nature of the heteroatom present on the helical shape.

Helicene chemistry¹ has grown into an important field of research owing to the fascinating optical² and electronic³ properties of these π -conjugated *ortho*-annelated aromatic molecules. Their inherent chirality has recently led to promising

applications in asymmetric catalysis,⁴ asymmetric molecular recognition,⁵ and liquid crystal molecules.⁶ In this context, the determination of the racemization barrier (RB) reflecting the repulsive interactions between terminal aromatic rings is a crucial helicity indicator. In the carbohelicene series, RBs are dependent on several factors such as the number of *ortho*-condensed rings, substitution at various helix sites, and the modulation of steric hindrance on the terminal positions of the inner helix.⁷ Thus, [4]helicenes become configurationally stable at room temperature with the introduction of a large sterical substituent upon the last cycle of the inner helix.⁸ Indeed, introduction of methyl substituents in the 1-position increased the stability of the configuration similarly to the effect of an additional ring.

Although an overview of the literature over the last century highlighted carbohelicenes as helical dominating frameworks, heterohelicenes (i.e., oxa-, aza-, and thiahelicene)⁹ recently emerged as extremely attractive molecules. Introduction of sulfur atoms revealed that they are especially beneficial to the electronic, optical, or photorefractive properties of thiahelicene-based material.¹⁰ Up to recently,

(1) For reviews, see: (a) Rajca, A.; Miyasaka, M. *Synthesis and Characterization of Novel Chiral Conjugated Materials*. In *Functional Organic Materials: Syntheses and Strategies*; Mueller, T. J. J., Bunz, U. H. F., Eds.; Wiley-VCH: Weinheim, Germany, 2007; pp 543–577. (b) Urbano, A. *Angew. Chem., Int. Ed.* **2003**, *42*, 3986–3989. (c) Katz, T. J. *Angew. Chem., Int. Ed.* **2000**, *39*, 1921–1923.

(2) (a) Wigglesworth, T. J.; Sud, D.; Norsten, T. B.; Lekhi, V. S.; Branda, N. R. *J. Am. Chem. Soc.* **2005**, *127*, 7272–7273. (b) Botek, E.; Champagne, B.; Turki, M.; André, J.-M. *J. Chem. Phys.* **2004**, *120*, 2042–2048. (c) Nuckolls, C.; Katz, T. J.; Verbiest, T.; Van Elshocht, S.; Kuball, H.-G.; Kiesewalter, S.; Lovinger, A. J.; Persoons, A. *J. Am. Chem. Soc.* **1998**, *120*, 8656–8660.

(3) (a) Furche, F.; Ahlrichs, R.; Wachsmann, C.; Weber, E.; Sobanski, A.; Vögtle, F.; Grimme, S. *J. Am. Chem. Soc.* **2000**, *122*, 1717–1724. (b) Treboux, G.; Lapstun, P.; Wu, Z.; Silverbrook, K. *Chem. Phys. Lett.* **1999**, *301*, 493–497. (c) Beljonne, D.; Shuai, Z.; Brédas, J. L.; Kauranen, M.; Verbiest, T.; Persoons, A. *J. Chem. Phys.* **1998**, *108*, 1301–1304.

(4) (a) Sato, I.; Yamashima, R.; Kadowaki, K.; Yamamoto, J.; Shibata, T.; Soai, K. *Angew. Chem., Int. Ed.* **2001**, *40*, 1096–1098. (b) Dreher, S. D.; Katz, T. J.; Lam, K. C.; Rheingold, A. L. *J. Org. Chem.* **2000**, *65*, 815–822. (c) Retz, M. T.; Sostmann, S. *J. Organomet. Chem.* **2000**, *603*, 105–109. (d) Okubo, H.; Yamaguchi, M.; Kabuto, C. *J. Org. Chem.* **1998**, *63*, 9500–9509. (e) Retz, M. T.; Beutenmüller, E. W.; Goddard, R. *Tetrahedron Lett.* **1997**, *38*, 3211–3214. (f) Aloui, A.; El Abed, R.; Marinetti, A.; Ben Hassine, B. *Tetrahedron Lett.* **2007**, *48*, 2017–2020.

(5) (a) Retz, M. T.; Sostmann, S. *Tetrahedron* **2001**, *57*, 2515–2520. (b) Murguly, E.; McDonald, R.; Branda, N. R. *Org. Lett.* **2000**, *2*, 3169–3172. (c) Weix, D. J.; Dreher, S. D.; Katz, T. J. *J. Am. Chem. Soc.* **2000**, *122*, 10027–10032. (d) Owens, L.; Thilgen, C.; Diederich, F.; Knobler, C. B. *Helv. Chim. Acta* **1993**, *76*, 2757–2774. (e) Yamamoto, K.; Ikeda, T.; Kitsuki, T.; Okamoto, Y.; Chikamatsu, H.; Nakazaki, M. *J. Chem. Soc., Perkin Trans. 1* **1990**, 271–276. (f) Xu, Y.; Zhang, X. Y.; Sugiyama, H.; Umamo, T.; Osuga, H.; Tanaka, K. *J. Am. Chem. Soc.* **2004**, *126*, 6566–6567. (g) Honzawa, S.; Okubo, H.; Anzai, S.; Yamaguchi, M.; Tsumoto, K.; Kumagai, I. *Bioorg. Med. Chem.* **2002**, *10*, 3213–3218.

(6) Nuckolls, C.; Katz, T. J. *J. Am. Chem. Soc.* **1998**, *120*, 9541–9544. (7) (a) Janke, R. H.; Haufe, J. H.; Würthwein, E.-U.; Borkent, J. H. *J. Am. Chem. Soc.* **1996**, *118*, 6031–6035. (b) Martin, R. H.; Marchant, M. J. *Tetrahedron* **1974**, *30*, 347–349.

(8) (a) Latorre, A.; Urbano, A.; Carreno, M. C. *Chem. Commun.* **2009**, 6652–6654. (b) Carreno, M. C.; Enriquez, A.; García-Cerrada, S.; Sanz-Cuesta, M. J.; Urbano, A.; Maseras, F.; Nonell-Canals, A. *Chem.—Eur. J.* **2008**, *14*, 603–620. (c) Laleu, B.; Mobian, P.; Herse, C.; Laursen, B. W.; Hopfgartner, G.; Bernardinelli, G.; Lacour, J. *Angew. Chem., Int. Ed.* **2005**, *44*, 1879–1883. (d) Herse, C.; Bas, D.; Krebs, F. C.; Burgi, T.; Weber, J.; Wesolowski, T.; Laursen, B. W.; Lacour, J. *Angew. Chem., Int. Ed.* **2003**, *42*, 3162–3166. (e) Carreno, M. C.; García-Cerrada, S.; Sanz-Cuesta, M. J.; Urbano, A. *Chem. Commun.* **2001**, 1452–1453.

(9) (a) For recent review, see: Dumitrescu, F.; Dumitrescu, D., G.; Aron, I. *ARKIVOC* **2010**, *1*, 1–32. (b) Rajca, A.; Pink, M.; Xiao, S.; Miyasaka, M.; Rajca, S.; Das, K.; Plessel, K. *J. Org. Chem.* **2009**, *74*, 7504–7513. (c) Miyasaka, M.; Pink, M.; Rajca, S.; Rajca, A. *Angew. Chem., Int. Ed.* **2009**, *48*, 5954–5957. (d) Tanaka, K.; Fukawa, N.; Suda, T.; Noguchi, K. *Angew. Chem., Int. Ed.* **2009**, *48*, 5470–5473. (e) Graule, S.; Rudolph, M.; Vanthuyne, N.; Autschbach, J.; Roussel, Ch.; Crassous, J.; Reau, R. *J. Am. Chem. Soc.* **2009**, *131*, 3183–3185. (f) Adriaenssens, L.; Severa, L.; Sálavá, T.; Cisarová, I.; Pohl, R.; Saman, D.; Rocha, S. V.; Finney, N. S.; Pospíšil, L.; Slavicek, P.; Teplý, F. *Chem.—Eur. J.* **2009**, *15*, 1072–1076. (g) Li, Ch.; Shi, J.; Xu, L.; Wang, Y.; Cheng, Y.; Wang, H. *J. Org. Chem.* **2009**, *74*, 408–411. (h) Collins, S. K.; Vachon, M. P. *Org. Biomol. Chem.* **2006**, *4*, 2518–2524. (i) Sato, K.; Katayama, Y.; Yamagishi, T.; Arai, S. *J. Heterocycl. Chem.* **2006**, *43*, 177–181. (j) Nakano, K.; Hidehira, Y.; Takahashi, K.; Hiyama, T.; Nozaki, K. *Angew. Chem.* **2005**, *117*, 7298–7300.

(10) Maiorana, S.; Papagni, A.; Licandro, E.; Annunziata, R.; Paravidino, P.; Perdicchia, D.; Giannini, C.; Bencini, M.; Clays, K.; Persoons, A. *Tetrahedron* **2003**, *59*, 6481–6488.

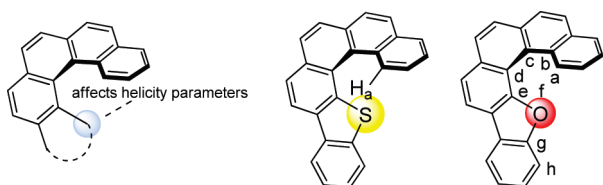
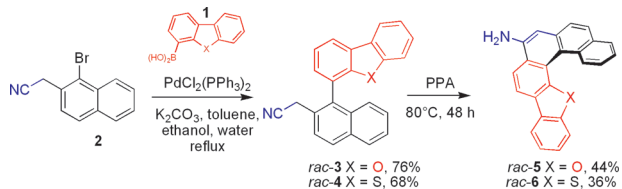


FIGURE 1. Targeted modulation at the end of the inner helix.

SCHEME 1. Synthesis of [5]Oxa- and [5]Thiahehelicenes (**5** and **6**)



heteroatoms embedded in heterohelicenes were located only at the outer framework of the helix.⁹

To the best of our knowledge, thiahehelicene comprising a sulfur atom at an inner helix position has been reported once and obtained through photocyclization strategy.¹¹ In this case, the presence of the sterically demanding sulfur atom at the end of the inner helix was shown to impact the degree of twisting into the heterohelicene.

The synthesis of regio-defined heterohelicenes is of significant current interest. Indeed the presence, the nature, and the position of heteroatoms may tune helicity parameters such as dihedral angles and bond lengths that modify the configurational stability such as the RB, thus affecting the potential applications in material science.

Herein we report the selective synthesis of unprecedented [5]oxa- and [5]thiahehelicenes (see Figure 1) where both oxygen and sulfur atoms are located at the end of the inner helix. In addition, we describe the determination of their respective RBs and highlight the crucial influence of the nature of the heteroatom on the helical shape and RB. The present route to heterohelicenes is based on our recent success in obtaining diamino[6]carbohelicenes by a short five-step sequence.¹² Target compounds **5** and **6** were obtained in two steps starting from the same intermediate **2** according to Scheme 1.

The preparation of the [5]oxahehelicene **5** and the [5]thiahehelicene **6** started from bromonaphthalene **2** and commercial boronic acids **1**.¹³ The Suzuki cross-coupling reaction was performed with PdCl₂TPP₂ and K₂CO₃ in a refluxing mixed solvent system of toluene/EtOH/H₂O.¹⁴ After purification by flash chromatography, the desired compounds **3** and **4** were, respectively, obtained in 76 and 68% yield. Nitriles **3** and **4** poured in PPA and heated at 80 °C for 48 h gave the corresponding helicenes **5** and **6**. Due to the unprecedented presence of heteroatoms at the end of the inner helix, complete NMR characterization is not trivial and required complementary analyses. Full assignments of

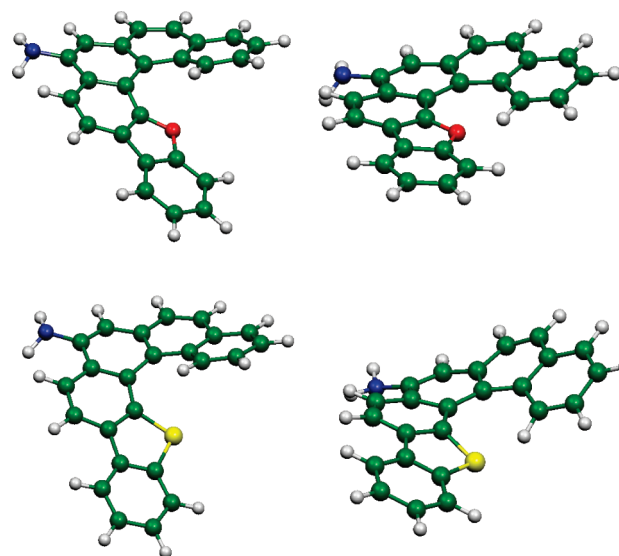


FIGURE 2. B3LYP/6-311+G(d,p) optimized minimum (left) and transition state structures (right) of [5]oxahehelicene **5** (top) and [5]thiahehelicene **6** (bottom).

all ¹H and ¹³C NMR signals highlighted the remarkable influence of the heteroatom, in particular on the chemical shifts of the closest h proton and g carbon atoms in both structures.

We evaluated and compared the helicity parameters of both [5]heterohelicenes **5** and **6**. Quantum chemical calculations were conducted to explore the geometries and electronic structures of the newly synthesized molecules as well as the pathway for interconversion between two enantiomers (racemization). All calculations were performed using Gaussian 03.¹⁵ The stationary state geometry of each structure (minimum or transition state for interconversion) has been optimized without symmetry constraints in the gas phase with density functional theory (DFT) method. We have used the B3LYP functional¹⁶ with the 6-311G+(d) triple- ζ polarized basis sets that provide accurate ground state structure for most organic systems.

The transition state (TS) structures for helicene racemization are shown in Figure 2 (right side). Interestingly, the TS structures found for **5** are nearly planar, while the geometry found for **6** is nonplanar with face-to-face orientation of the terminal aromatic rings. A close X...H_a contact between X and H atoms occurs in the crowded concave region of the molecule where the nuclei of these two atoms are separated by 1.800 and 2.084 Å in the **5** and **6** optimized geometries.

These distances are significantly shorter than twice the van der Waals radius of the hydrogen atom and sulfur or oxygen atoms (2.72 and 3.00 Å, respectively). Therefore, the strong repulsive interaction established in the TS of racemization for **5** is balanced by the planar geometry that provides a significant stabilization of the transition state structure and thus explains the low RB value.

The computed RB values show that the energy barrier is strongly dependent on the molecular structure and the nature of introduced heteroatom. Indeed, for oxahehelicene

(11) Pietrangelo, A.; Patrick, B. O.; MacLachlan, M. J.; Wolf, M. O. *J. Org. Chem.* **2009**, *74*, 4918–4926.

(12) Pieters, G.; Gaucher, A.; Marrot, J.; Prim, D. *Chem. Commun.* **2009**, 4827–4828.

(13) Compound **2** was obtained in two steps from the commercially available 1-bromo-2-methylnaphthalene according to procedure described in ref 12.

(14) Whitaker, C. W.; McMahon, R. J. *J. Phys. Chem.* **1996**, *100*, 1881–1890.

(15) Frisch, M. J. et al. *GAUSSIAN 03*, revision D.01; Gaussian Inc.: Wallingford, CT, **2004**.

(16) Becke, A. D. *J. Chem. Phys.* **1993**, *98*, 5648–5665.

TABLE 1. Key Structural Parameters of [5]Heterohelicenes **5** and **6**

compound	dihedral angle ^a (°)			X...H _a distance (Å)
	a-b-c-d	b-c-d-e	c-d-e-f	
5 (X = O)				
minimum	-19.0	-26.3	-8.4	2.34
TS	8.8	-3.0	-9.5	1.80
6 (X = S)				
minimum	-20.8	-30.4	-13.9	2.76
TS	24.9	-9.0	-28.8	2.08

^aSee numbering reported in Figure 1.

derivative **5**, this energy barrier is found to be around 9 kcal/mol while it is considerably much higher for compound **6** (i.e., about 20 kcal/mol).

The optimized minima of [5]heterohelicenes **5** and **6** and transition states of racemization are displayed in Figure 2.

All six fused rings show distortion from planar arrangement, as evidenced by the dihedral angles between adjacent rings (Table 1). The spatial distortion of the backbone of the conjugated π system can also be revealed by the significant climb of the helices (X...H_a distance). In compound **6**, the X...H_a distance is longer and the dihedral angles are wider than those in compound **5**.

In conclusion, we succeeded in the first preparation of novel regio-defined [5]oxa- and [5]thiaheterohelicenes. These helical molecules were obtained through a short and facile two-step access in fair yields. The strategy described herein allowed the selective introduction of both oxygen and sulfur atoms at the end of the inner helix. The determination of helicity parameters and configurational stability evidenced that energy barriers are strongly dependent on the nature of the heteroatom introduced in the inner helix position. The latter deeply impacted both ground and transition state structures, confirming that increases of the heteroatom size and racemization barrier evolved parallel to one another.

Experimental Section

Representative Procedure for Suzuki–Miyaura Coupling. Synthesis of 1-(4-Dibenzofurane)-2-cyanomethylnaphthalene **3.** To a stirred suspension of 1-bromo-2-cyanomethylnaphthalene **2** (100 mg, 0.4 mmol), 4-dibenzofuranboronic acid (169 mg, 0.8 mmol, 2 equiv), and K₂CO₃ (168 mg, 1.2 mmol, 3 equiv) in degassed mixture of toluene (1 mL), absolute ethanol (0.2 mL) and water (0.2 mL) was added PdCl₂(PPh₃)₂ (29 mg, 0.04 mmol,

10% mol). The mixture was stirred at reflux for one night. Water (10 mL) was then added, and the aqueous phase was extracted with dichloromethane (2 × 10 mL). The combined organic layers were dried (MgSO₄), filtered, and concentrated under vacuum. The crude product was purified by flash chromatography on silica gel (petroleum ether/EtOAc: 97.5/2.5 then 95/5) to give the oxanitrile product **3** (103 mg, 76%) as a pale yellow solid: mp 138 °C; ¹H NMR (300 MHz, CDCl₃) δ = 3.66 (m, 2 H), 7.35–7.50 (m, 6 H), 7.55 (m, 2 H), 7.78 (d, *J* = 8.5 Hz, 1 H), 7.95 (d, *J* = 8.1 Hz, 1 H), 8.06 (d, *J* = 7.7 Hz, 2 H), 8.13 (dd, *J* = 7.1 and 1.3 Hz, 1 H); ¹³C NMR (300 MHz, CDCl₃) δ = 22.4, 111.8, 117.9, 120.7, 120.9, 121.2, 123.0, 123.2, 123.9, 124.8, 125.6, 126.1, 126.3, 126.6, 126.8, 127.5, 128.1, 129.1, 129.4, 132.5, 132.9, 133.0, 153.8, 156.1; IR (KBr) 3057, 2361 (CN), 1631, 1449, 1410, 1188, 1115, 754 cm⁻¹; HRMS-ESI *m/z* [M + H]⁺ calcd for C₂₄H₁₆NO 334.1232, found 334.1217.

Representative Procedure for Cyclization. Synthesis of 7-Amino-5-oxahelicene **5.** The oxanitrile product **3** (30 mg, 0.11 mmol) was poured into stirred fresh polyphosphoric acid (3 mL) at 80 °C under argon. The suspension was stirred at 80 °C for 48 h. The resulting mixture was poured into ice (20 g) and basified with Na₂CO₃. This aqueous layer was extracted with ethyl acetate (3 × 10 mL), and the combined organic layers were dried (MgSO₄), filtered, and concentrated under vacuum. The crude product was purified by flash chromatography on silica gel (dichloromethane) to give 7-amino-[5]-oxahelicene **5** (13 mg, 44%) as a red solid: mp 142 °C; ¹H NMR (300 MHz, CD₂Cl₂) δ = 4.46 (br s, 2 H), 7.13 (s, 1 H), 7.60–7.35 (m, 5 H), 7.68 (d, *J* = 8.6 Hz, 1 H), 7.90 (d, *J* = 8.5 Hz, 1 H), 7.96 (dd, *J* = 8.1 and 1.8 Hz, 1 H), 8.02 (d, *J* = 8.5 Hz, 1 H), 8.11 (m, 1 H), 8.26 (d, *J* = 8.5 Hz, 1 H), 8.38 (dd, *J* = 8.6 and 1.0 Hz, 1 H); ¹³C NMR (75 MHz, CD₂Cl₂) δ = 108.0, 111.2, 116.2, 117.5, 117.9, 118.3, 119.8, 121.1, 122.6, 123.8, 124.0, 124.4, 124.8, 124.9, 126.5, 126.9, 128.1, 128.6, 129.7, 131.1, 133.0, 141.3, 152.4, 154.3; IR (neat) 3345, 3224, 3044, 2155, 1627, 1591, 1454, 1190 cm⁻¹; HRMS-ESI *m/z* [M + Na]⁺ calcd for C₂₄H₁₅NONa 356.1051, found 356.1032.

Acknowledgment. Authors gratefully thank MENRT, CNRS, and the University of Versailles-St-Quentin-en-Yvelines for a grant (G.P.) and financial support.

Supporting Information Available: Experimental procedures, full 1D and 2D NMR characterization data in DMF, full geometry and energy information in the form of GAUSSIAN 03 archive entries. This material is available free of charge via the Internet at <http://pubs.acs.org>.